OPEN ACCESS
Saudi Journal of Civil Engineering
Abbreviated Key Title: Saudi J Civ Eng
ISSN 2523-2657 (Print) |ISSN 2523-2231 (Online)
Scholars Middle East Publishers, Dubai, United Arab Emirates
Journal homepage: http://saudijournals.com/sjce/

Original Research Article

Analysis of Penetration Mechanical Characteristics of Multi-layer Civil Engineering Materials

Yanhua She*

School of Urban Construction, Yangtze University, Jingzhou, China

DOI: 10.36348/sjce.2020.v04i09.001 | **Received:** 06.10.2020 | **Accepted:** 02.11.2020 | **Published:** 05.11.2020

***Corresponding author:** Yanhua She

Abstract

According to the three-layer airport runway, based on spherical cavity-expansion theory and considering interface effect of concrete-macadam-soil by analyzing kinetic energy projectile penetrating layered target of concrete-macadam-soil, penetration models of concrete cratering, concrete pore-forming, macadam pore-forming and soil pore-forming are established. In addition, numerical solution of control equations is carried out by using Runge-Kutta method. And the Time-history curve of residual velocity is obtained. The theoretical analysis shows that because of the interface effect, the penetration resistance of projectile suffered on concrete layer and macadam layer when moving , is related not only to penetration velocity, mass, projectile shape and medium character, but also to penetration depth, which is the biggest difference compared with penetrating into single layer. Finally, by means of finite element simulation, the process of oblique penetrating into multilayered medium of airport runway is simulated by three dimensional numerical analysis. Thus, the influence of the penetration velocity and the boundary of the runway on the penetration process were studied. The results show that the presence of the multi-layer media interface of the runway accelerates the attitude of the projectile body; the smaller the penetration rate is, the more obvious the phenomenon is. At the same time, the overload response of projectile body is changed. The research results have laid a foundation for the further research on the technology of the composite medium penetration into the airport runway. They also have reference value for the research on the failure of civil engineering materials under the action of dynamic loads.

Keywords: Penetration, Multi-layer target, Concrete, Macadam, Soil, Simulation.

INTRODUCTION

Air force aviation operations, training, exercises and all combat readiness activities are inseparable from the airport. The security of the airport is of great strategic significance. Airport runway is composed of concrete-macadam-soil composite medium. Because of its particularity structure, the protection ability of these kind of military targets is also constantly strengthened and improved. To understand and master the penetration law of kinetic energy penetration projectile into the targets composed of concrete macadam soil composite medium, and to further improve the penetration ability and damage efficiency of kinetic energy penetration projectile against such targets have become urgent problems to be solved in modern warfare.

Over the past decades, scholars have conducted systematic and in-depth theoretical analysis and experimental research on the penetration of kinetic energy projectiles, and achieved rich results. The penetration of kinetic projectiles is a very complex mechanical problem. Theoretical analysis combined with experiment and numerical calculation is an important approach to penetration research. In the 1970s, SNL put forward the cylindrical cavity expansion theory (CCET) and spherical cavity-expansion theory (SCET) for incompressible materials [1]. Since then, numerous articles using SCET and CCET to estimate penetration depth have appeared. Forrestal [2-5] successively put forward cavity expansion models for rock, soil, concrete and other materials. Gao *et al*. [6] based on the equation of the dynamic behavior of materials under high speed and high pressure, established the equation of the general curved surface before the corresponding shock wave, and put forward the so-called normal expansion theory for concrete materials. Wang *et al*. [7] adopted the unified strength theory as the yield criterion of concrete materials, and provided the theoretical calculation formula for the penetration depth of oval projectile under the condition of cylindrical cavity expansion. Lin

et al. [8] proposed a spherical cavity expansion theory taking into account the interface effect of soil concrete by using Euler method. Meng *et al*. [9] proposed a finite dynamic spherical cavity-expansion approximation model with radially elastic confinement to analyze the confinement on concrete targets and predict the depth of penetration (DOP). However, there are few theoretical studies on the penetration of kinetic energy projectiles into multi-layer composite media such as airport runway. In this paper, the spherical cavity expansion model of a three-layer composite airstrip is established considering the interface effect.

Theoretical Analysis of Penetrating Composite Media

Hypothesis

The cavity expansion theory is the basis of the research on kinetic energy penetrating projectile penetrating concrete macadam soil composite medium. So based on the theory of spherical cavity expansion, the stress relationship between the elastic response zone and the plastic response zone is discussed, and then expression of radial stress on cavity surface is obtained. Therefore, it makes the following hypothesis:

1. Concrete and macadam medium are isotropic and homogeneous elastic-plastic materials with finite thickness.
2. Soil medium is isotropic, homogeneous elastic-plastic materials elastic-plastic materials with Semi-infinite.
3. Each response zone is spherically symmetric.

As shown in Fig.1, spherically symmetric cavity expands at a constant velocity V from the initial zero radiuses to outside. Plastic and elastic response zones are generated during expansion. The plastic region is the region surrounded by radii r=Vt and r=ct. r is the radial coordinate in Euler spherical coordinates. t is time, c is the velocity of the elastic-plastic interface, and the elastic region is the region of r>ct.

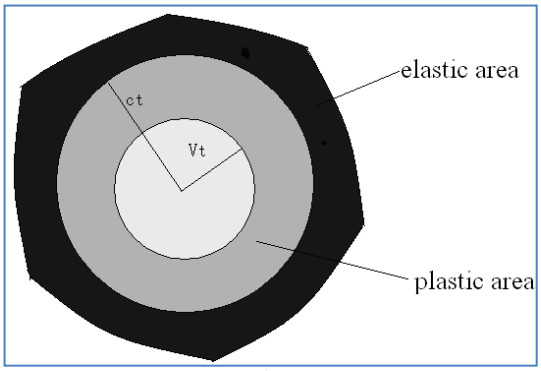

Fig-1: Response Area of Elasticity and Plasticity

4. Concrete-macadam-soil are incompressible materials, bend rule serving the Mohr-Coulomb criterion [6].

$$\sigma = \frac{1}{3}(\sigma_r + \sigma_\theta + \sigma_\phi) \qquad \sigma_\theta = \sigma_\phi \tag{1}$$

$$\sigma_r - \sigma_\theta = \lambda\sigma + \tau \qquad \tau = [(3-\lambda)/3]\sigma_c \tag{2}$$

In the two equations above, σ is hydrostatic pressure, σ_r, σ_θ and σ_ϕ are Cauchy Radial stress, λ is material intensify modulus, τ is yield limitation, σ_c is uniaxial compressive strength.

The response of the composite medium

According to the relative positions of the elastoplastic interface and the interface between the concrete macadam and the soil in the concrete macadam soil composite medium, the cavities in the composite medium can be divided into the following eight states (Fig. 2).

a) The response of the composite medium before the elastic-plastic interface reaches the concrete macadam interface;
b) The response of the composite medium when the elastoplastic interface reaches the interface of the concrete macadam soil and the macadam has not yet yielded;
c) The response of the composite medium when the elastoplastic interface reaches the interface of the concrete macadam soil and the macadam has yielded;
d) The response of the composite medium when the expansion surface is located in the concrete medium and the elastic-plastic interface reaches the interface between soil and macadam and the soil medium has not yet yielded;
e) The response of the composite medium when the cavity expansion surface is located in the concrete medium and the soil medium begins to yield;
f) The response of the composite medium when the cavity expansion surface reaches the macadam layer and the elastic-plastic interface has not reached the macadam soil interface;
g) The response of the composite medium when the cavity expands to the macadam layer and the elastic-plastic interface reaches the interface between the macadam and the soil and the soil has not yet yielded;
h) The response of the composite medium when the cavity expansion surface moves to the macadam layer and the soil begins to yield.

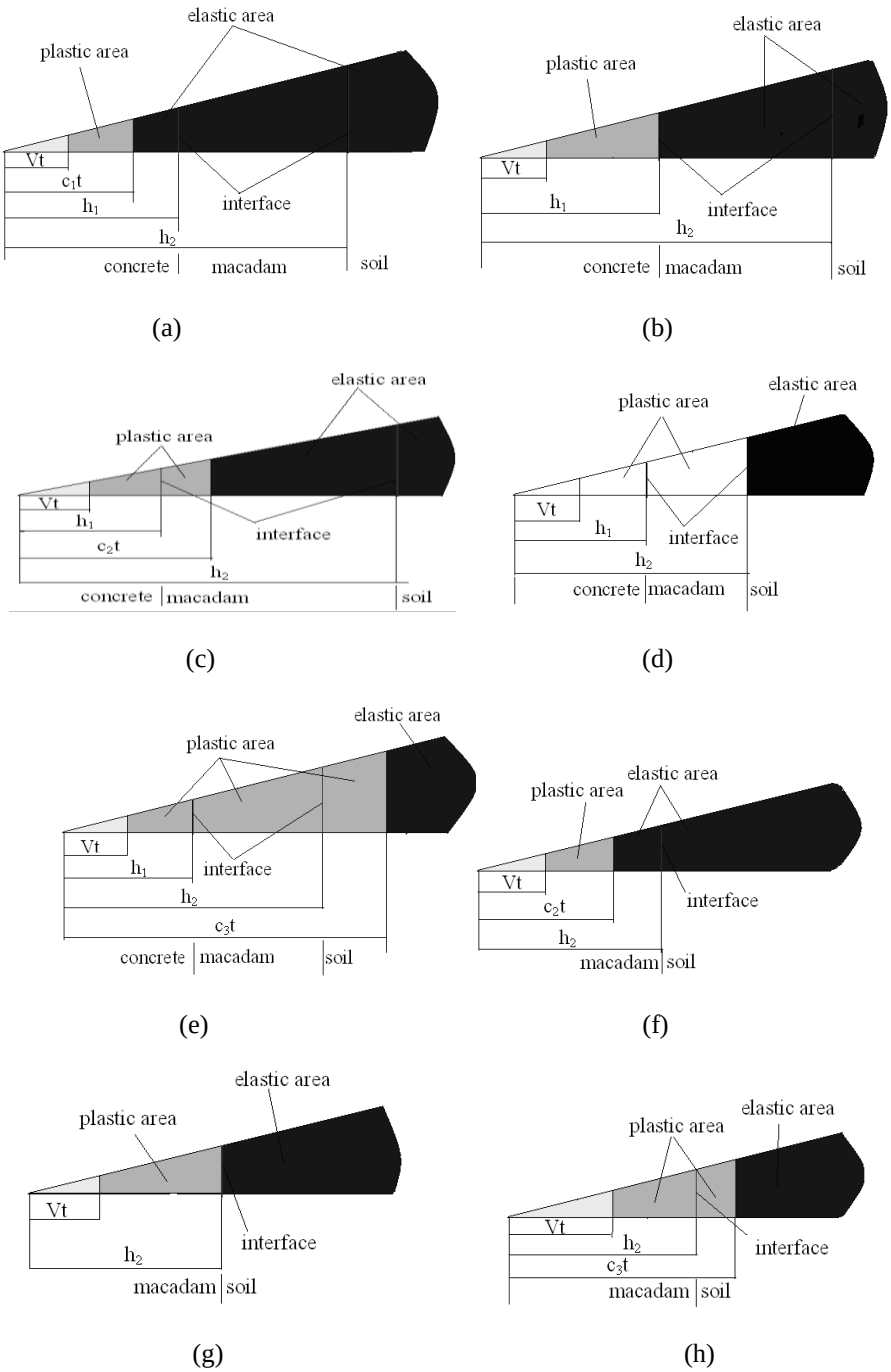

Fig-2: Response state

Penetration model analysis

The penetration process of kinetic penetration projectile into concrete, macadam and soil is very complicated. It includes two penetration processes of medium resistant concrete and macadam, and low resistant soil. The penetration process can be divided into four stages: pit and pore formation in concrete layer, pore formation in macadam layer and pore formation in soil layer. Therefore, the penetration model of kinetic penetration projectiles into the concrete-macadam-soil composite media can be established according to the above four stages. To simplify the problem, the following assumptions are made:

1. The tangential oval projectile penetrates into the concrete macadam soil composite target plate vertically;
2. During penetration, the projectile remains rigid, and the friction between the warhead and the projectile body is ignored;
3. The normal pressure distribution of the warhead part in the perforation stage conforms to the radial stress distribution law of the cavity surface in the spherical cavity expansion theory, and the velocity of the cavity is equal to the component of the particle on the surface perpendicular to the warhead part.

The penetration model is shown in Fig. 3:

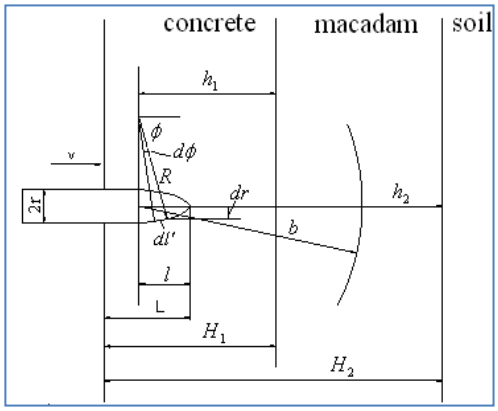

Fig-3: Penetration model

In Fig.3, r is the radius of the kinetic penetration projectile; R is head arc radius of the kinetic penetration projectile; l is warhead length; L is penetration depth; b is radius of plastic zone; h_1 is The distance from the concrete-macadam interface to the bottom of the warhead; h_2 is the distance from the macadam-soil interface to the bottom of the warhead; H_1 is the distance from the concrete-macadam interface to the free surface; H_2 is the distance from the macadam-soil interface to the free surface, ϕ is the shape of the oval projectile head and it is usually represented by CRH (caliber-radius-head): $CRH = R/d = \phi$.

Based on the spherical cavity expansion theory, the penetration models in the perforation stage and the pit formation stage are established as follows.

Perforation stage model

The positive pressure on the micro ring dl' of the penetrating warhead is:

$$dF = 2\pi \cdot dr \cdot dl' \cdot \sigma_n(V_L, \phi) \tag{3}$$

Then the axial resistance on the dl' when the projectile penetrating is:

$$dF_L = 2\pi \cdot dr \cdot dl' \cdot \sigma_n(V_L, \phi)\cos\phi \tag{4}$$

It can be obtained from the geometric relationship in Fig.3,

$$dr = r - R + R\sin\phi, \qquad dl' = Rd\phi \tag{5}$$

Substitute Eq. (5) into Eq. (4) to get

$$dF_L = 2\pi R^2\left[\sin\phi - \left(\frac{R-r}{R}\right)\right]\cdot\sigma_n(V_L,\phi)\cdot\cos\phi\cdot d\phi \tag{6}$$

Then, the resistance acting on the kinetic energy penetrating the warhead during the pore formation stage of concrete-macadam and soil is given by the following equations:

$$F_L = 2\pi R^2\int_{\phi_0}^{\pi/2}\left[\sin\phi - \left(\frac{R-r}{R}\right)\right]\cdot\cos\phi\cdot\sigma_n(V_L,\phi)d\phi \tag{7}$$

$$\phi_0 = sin^{-1}\left(\frac{R-r}{R}\right) \tag{8}$$

In Eq.(7), $\sigma_n(V_L,\phi)$ is the positive stress acting on the kinetic energy penetrating warhead; V_L is the penetration velocity. The relation between V_L and the expansion velocity of the spherical cavity is

$$V = V_L\cos\phi \tag{9}$$

That's known from the hypothesis, there are

$$\sigma_n(V_L,\phi) = \tau_{0i}S \tag{10}$$

$$S = \frac{\sigma_r}{\tau_{0i}} = A + B\rho_i V_L{}^2/\tau_{0i} \tag{11}$$

In Eq. (11), S is the dimensionless stress on the surface of the cavity.

By substituting Eq.(8)(9)(10)(11) into Eq. (7), the integral can be obtained as follows:

$$F_L = C_A + C_B\cdot V_L{}^2 \tag{12}$$

$$C_A = \pi r^2\tau_{0i}A \tag{13}$$

$$C_B = \pi r^2 \rho_i B \frac{8\psi - 1}{24\psi^2} \quad (\psi = \frac{R}{2r}) \tag{14}$$

In above equations, A and B are the quantity related to the properties of concrete-macadam-soil composite medium material and the response state in the medium.

The kinetic energy projectile penetrating the projectile for rigid body motion is given by Newton's second law

$$m\frac{d^2L}{dt^2} = -(C_A + C_B \cdot V_L^2) \tag{15}$$

It can be seen that as long as the relationships between the parameters A and B are determined, the penetration rule of the kinetic projectile penetrating into the concrete- macadam- soil composite medium can be obtained.

Before kinetic energy projectile entering the macadam layer

(1) Before the elastoplastic interface reaches the concrete-macadam interface, it is expressed by the geometric relationship

$$h_1 = H_1 - L + l \tag{16}$$

The condition before the elastic-plastic interface reaches the interface between concrete and macadam is

$$b + L - l \le H_1 \tag{17}$$

Because r = ε_1b ($\varepsilon_i = \frac{V}{c_i}$), if the penetration depth is L^1 when the elastic-plastic interface reaches the concrete-macadam interface, then Eq. (17) can be rewritten as

$$L \le L^1 = H_1 + l - r/\varepsilon_1 \tag{18}$$

And the dimensionless radial stresses on the surface of the cavity is as follows

$$\left.\begin{aligned} S &= A + B\rho_1 V^2/\tau_{01} \\ A &= -\frac{1}{\lambda_1} + \varepsilon_1^{-\alpha_1\lambda_1}\left(\frac{1}{\lambda_1} + \frac{2}{3} + \frac{2}{3E_1}\left[\frac{r}{\varepsilon_1 h_1}\right]^3 (E_2 - E_1) + \frac{2}{3E_1}\left[\frac{r}{\varepsilon_1 h_2}\right]^3 (E_3 - E_2)\right) \\ B &= -\frac{2}{(\alpha_1\lambda_1 - 1)} + \frac{2}{(\alpha_1\lambda_1 - 4)} + \\ &\left\{\frac{2\varepsilon_1}{(\alpha_1\lambda_1 - 1)} - \frac{2\varepsilon_1^4}{(\alpha_1\lambda_1 - 4)} + \frac{3\tau_{01}}{\rho_1 E_1}\left[\rho_1 + \frac{r}{\varepsilon_1 h_1}(\rho_2 - \rho_1) + \frac{r}{\varepsilon_1 h_2}(\rho_3 - \rho_2)\right]\right\}\varepsilon_1^{-\alpha_1\lambda_1} \end{aligned}\right\} \tag{19}$$

Among them $\alpha_i = \frac{6}{3 + 2\lambda_i}$

(2) The elastic-plastic interface reaches the concrete- macadam interface, and the condition that the macadam medium does not yield is

$$L^1 < L < L^2 \tag{20}$$

There $L^2 = H_1 + l - r/\varepsilon_2$ is the penetration depth when the macadam medium begins to yield.

The dimensionless radial stress on the cavity surface is

$$\left.\begin{aligned} S &= A + B\rho_1 V^2/\tau_{01} \\ A &= -\frac{1}{\lambda_1} + \left(\frac{h_1}{r}\right)^{\alpha_1\lambda_1}\left[\frac{1}{\lambda_1} + \frac{4E_2}{9\tau_{01}}\left(\frac{r}{h_1}\right)^3 + \frac{4}{9\tau_{01}}\left(\frac{r}{h_2}\right)^3 (E_3 - E_2)\right] \\ B &= -\frac{2}{(\alpha_1\lambda_1 - 1)} + \frac{2}{(\alpha_1\lambda_1 - 4)} + \left(\frac{h_1}{r}\right)^{\alpha_1\lambda_1}\left[\frac{1}{(\alpha_1\lambda_1 - 1)} \cdot \frac{2r}{h_1} - \frac{2}{(\alpha_1\lambda_1 - 4)} \cdot \left(\frac{r}{h_1}\right)^4\right. \\ &\left. + \frac{\rho_2}{\rho_1}\frac{2r}{h_1} + \frac{1}{\rho_1}\frac{2r}{h_2}(\rho_3 - \rho_2)\right] \end{aligned}\right\} \tag{21}$$

(3) When the elastic-plastic interface reaches the macadam-soil interface after the macadam medium begins to yield, the condition that should be satisfied is

$$L^2 < L < L^3 \tag{22}$$

Where $L^3 = l + H_2 - r/\varepsilon_2$ is the penetration depth when the elastic-plastic interface reaches the macadam-soil interface?

Accordingly, the dimensionless radial stress on the cavity surface is

$$\left.\begin{aligned} S &= A + B\rho_2 V^2/\tau_{02} \\ A &= -\frac{1}{\lambda_1}\frac{\tau_{01}}{\tau_{02}} + \left(\frac{h_1}{\varepsilon_2 b}\right)^{\alpha_1\lambda_1}\left[-\frac{1}{\lambda_2} + \frac{1}{\lambda_1}\frac{\tau_{01}}{\tau_{02}} + \left(\frac{2}{3} + \frac{2}{3E_2}\left(\frac{b}{h_2}\right)^3(E_3 - E_2) + \frac{1}{\lambda_2}\right)\left(\frac{h_1}{b}\right)^{-\alpha_2\lambda_2}\right] \\ B &= -\frac{2\rho_1}{\rho_2(\alpha_1\lambda_1 - 1)} + \frac{2\rho_1}{\rho_2(\alpha_1\lambda_1 - 4)} + \left(\frac{h_1}{\varepsilon_2 b}\right)^{\alpha_1\lambda_1}\left\{\frac{b}{h_1}\left[\frac{2\rho_1\varepsilon_2}{\rho_2(\alpha_1\lambda_1 - 1)} - \frac{2\varepsilon_2}{\alpha_2\lambda_2 - 1}\right]\right. \\ &\quad + \left(\frac{b}{h_1}\right)^4\left[\frac{2\varepsilon_2^4}{(\alpha_2\lambda_2 - 4)} - \frac{2\rho_1\varepsilon_2^4}{\rho_2(\alpha_2\lambda_2 - 4)}\right] + \left(\frac{h_1}{b}\right)^{-\alpha_2\lambda_2}\left[\frac{3\tau_{02}}{\varepsilon_2^2 E_2} + \frac{3\tau_{02}b}{E_2\varepsilon_2^2 h_2}\frac{1}{\rho_2}(\rho_3 - \rho_2)\right. \\ &\quad \left.\left. + \frac{2\varepsilon_2}{\alpha_2\lambda_2 - 1} - \frac{2\varepsilon_2^4}{\alpha_2\lambda_2 - 4}\right]\right\} \end{aligned}\right\} \tag{23}$$

(4) The elastic-plastic interface reaches macadam-soil interfac, and the soil begins to yield

①When $L^3 < L < L^4$, ($L^4 = l + H_2 - r/\varepsilon_3$ is the penetration depth when the soil medium begins to yield), The dimensionless radial stress on the cavity surface is

$$\left.\begin{aligned} S &= A + B\rho_2 V^2/\tau_{02} \\ A &= -\frac{1}{\lambda_1}\frac{\tau_{01}}{\tau_{02}} + \left(\frac{h_1}{Vt}\right)^{\alpha_1\lambda_1}\left\{\frac{1}{\lambda_1}\frac{\tau_{01}}{\tau_{02}} - \frac{1}{\lambda_2} + \left(\frac{h_2}{h_1}\right)^{\alpha_2\lambda_2}\left[\frac{1}{\lambda_2} + \frac{4E_3}{9\tau_{02}}\left(\frac{Vt}{h_2}\right)^3\right]\right\} \\ B &= \frac{2\rho_1}{\rho_2(\alpha_1\lambda_1 - 1)} + \frac{2\rho_1}{\rho_2(\alpha_1\lambda_1 - 4)}\left(\frac{h_1}{a}\right)^{\alpha_1\lambda_1}\left\{\frac{2}{\rho_2}\cdot\frac{Vt}{h_1}\left(\frac{\rho_1}{\alpha_1\lambda_1 - 1} - \frac{\rho_2}{\alpha_2\lambda_2 - 1}\right)\right. \\ &\quad + \frac{2}{\rho_2}\cdot\left(\frac{Vt}{h_1}\right)^4\left(\frac{\rho_2}{\alpha_2\lambda_2 - 4} - \frac{\rho_1}{\alpha_1\lambda_1 - 4}\right) + \left(\frac{h_2}{h_1}\right)^{\alpha_2\lambda_2}\left[\frac{2}{\rho_2}\cdot\frac{Vt}{h_2}\left(\rho_3 + \frac{\rho_2}{\alpha_2\lambda_2 - 1}\right)\right. \\ &\quad \left.\left. - \frac{2}{(\alpha_2\lambda_2 - 4)}\cdot\left(\frac{Vt}{h_2}\right)^4\right]\right\} \end{aligned}\right\} \tag{24}$$

②When $L^4 < L < H_1$, the dimensionless radial stress on the cavity surface is

$$\left.\begin{aligned} S &= A + B\rho_3 V^2/\tau_{03} \\ A &= -\frac{1}{\lambda_1}\frac{\tau_{01}}{\tau_{03}} + \left(\frac{h_1}{b\varepsilon_3}\right)^{\alpha_1\lambda_1}\left\{\frac{1}{\lambda_1}\frac{\tau_{01}}{\tau_{03}} - \frac{1}{\lambda_2}\frac{\tau_{02}}{\tau_{03}} + \left(\frac{h_2}{h_1}\right)^{\alpha_2\lambda_2}\left[\frac{1}{\lambda_2}\frac{\tau_{02}}{\tau_{03}} - \frac{1}{\lambda_3} + \left(\frac{b}{h_2}\right)^{\alpha_3\lambda_3}\left(\frac{2}{3} + \frac{1}{\lambda_3}\right)\right]\right\} \\ B &= \frac{2\rho_1}{\rho_3(\alpha_1\lambda_1 - 1)} + \frac{2\rho_1}{\rho_3(\alpha_1\lambda_1 - 4)} + \left(\frac{h_1}{b\varepsilon_3}\right)^{\alpha_1\lambda_1}\left\{\frac{2\varepsilon_3}{\rho_3}\cdot\frac{b}{h_1}\left(\frac{\rho_1}{\alpha_1\lambda_1 - 1} - \frac{\rho_2}{\alpha_2\lambda_2 - 1}\right)\right. \\ &\quad + \frac{2\varepsilon_3^4}{\rho_3}\cdot\left(\frac{b}{h_1}\right)^4\left(\frac{\rho_2}{\alpha_2\lambda_2 - 4} - \frac{\rho_1}{\alpha_1\lambda_1 - 4}\right) + \left(\frac{h_2}{h_1}\right)^{\alpha_2\lambda_2}\left\{\frac{2\varepsilon_3}{\rho_3}\cdot\frac{b}{h_2}\left(\frac{\rho_2}{\alpha_2\lambda_2 - 1} - \frac{\rho_3}{\alpha_3\lambda_3 - 1}\right)\right. \\ &\quad \left.\left. + \frac{2\varepsilon_3^4}{\rho_3}\cdot\left(\frac{b}{h_2}\right)^4\left(\frac{\rho_3}{\alpha_3\lambda_3 - 4} - \frac{\rho_2}{\alpha_2\lambda_2 - 4}\right) + \left(\frac{b}{h_2}\right)^{\alpha_3\lambda_3}\left[\frac{3\tau_{03}}{\varepsilon_3^2 E_3} + \frac{2\varepsilon_3}{\alpha_3\lambda_3 - 1} - \frac{2\varepsilon_3^4}{\alpha_3\lambda_3 - 4}\right]\right\}\right\} \end{aligned}\right\} \tag{25}$$

Kinetic energy projectile have been entering the macadam layer

(1) Before the elastic-plastic interface reaches the macadam-soil interface, there is $H_2 < L < L_3$.

The dimensionless radial stress on the cavity surface is

$$\left.\begin{aligned} S &= A + B\rho_2 V^2/\tau_{02} \\ A &= -\frac{1}{\lambda_2} + \varepsilon_2^{-\alpha_2\lambda_2}\left(\frac{2}{3} + \frac{2}{3E_2}\left(\frac{b}{h_2}\right)^3 (E_3 - E_2) + \frac{1}{\lambda_2}\right) \\ B &= -\frac{2}{\alpha_2\lambda_2 - 1} + \frac{2}{\alpha_2\lambda_2 - 4} + \varepsilon_2^{-\alpha_2\lambda_2}\left(\frac{3\tau_{02}}{\varepsilon_2^2 E_2} + \frac{3\tau_{02} b}{\varepsilon_2^2 \rho_2 E_2 h_2}(\rho_3 - \rho_2) + \frac{2\varepsilon_2}{\alpha_2\lambda_2 - 1} - \frac{2\varepsilon_2^4}{\alpha_2\lambda_2 - 4}\right) \end{aligned}\right\} \quad (26)$$

(2) When the elastic-plastic interface reaches the macadam-soil interface and the soil has not yet yielded, $L^3 < L < L^4$.

The dimensionless radial stress on the cavity surface is

$$\left.\begin{aligned} S &= A + B\rho_2 V^2/\tau_{02} \\ A &= -\frac{1}{\lambda_2} + \left(\frac{h_2}{Vt}\right)^{\alpha_2\lambda_2}\left(\frac{1}{\lambda_2} + \frac{4E_3}{9\tau_{02}}\left(\frac{Vt}{h_2}\right)^3\right) \\ B &= -\frac{2}{\alpha_2\lambda_2 - 1} + \frac{2}{\alpha_2\lambda_2 - 4} + \left(\frac{h_2}{Vt}\right)^{\alpha_2\lambda_2}\left[\frac{2}{\rho_2}\cdot\frac{Vt}{h_2}\left(\rho_3 + \frac{\rho_2}{\alpha_2\lambda_2 - 1}\right) - \frac{2}{\alpha_2\lambda_2 - 4}\cdot\left(\frac{Vt}{h_2}\right)^4\right] \end{aligned}\right\} \quad (27)$$

(3) When the elastic-plastic interface reaches the macadam-soil interface and the soil has yielded, $L^4 < L < H_2$

The dimensionless radial stress on the cavity surface is

$$\left.\begin{aligned} S &= A + B\rho_3 V^2/\tau_{03} \\ A &= -\frac{1}{\lambda_1}\frac{\tau_{02}}{\tau_{03}} + \left(\frac{h_2}{b\varepsilon_3}\right)^{\alpha_2\lambda_2}\left[\frac{1}{\lambda_2}\frac{\tau_{02}}{\tau_{03}} - \frac{1}{\lambda_3} + \left(\frac{b}{h_2}\right)^{\alpha_3\lambda_3}\left(\frac{2}{3} + \frac{1}{\lambda_3}\right)\right] \\ B &= -\frac{2\rho_2}{\rho_3(\alpha_2\lambda_2 - 1)} + \frac{2\rho_2}{\rho_3(\alpha_2\lambda_2 - 4)} + \left(\frac{h_2}{b\varepsilon_3}\right)^{\alpha_2\lambda_2}\left\{\frac{2\varepsilon_3}{\rho_3}\cdot\frac{b}{h_2}\left(\frac{\rho_2}{\alpha_2\lambda_2 - 1} - \frac{\rho_3}{\alpha_3\lambda_3 - 1}\right)\right. \\ &\quad \left. + \frac{2\varepsilon_3^4}{\rho_3}\left(\frac{b}{h_2}\right)^4\left(\frac{\rho_3}{\alpha_3\lambda_3 - 4} - \frac{\rho_2}{\alpha_2\lambda_2 - 4}\right) + \left(\frac{b}{h_2}\right)^{\alpha_3\lambda_3}\left(\frac{3\tau_{03}}{\varepsilon_3^2 E_3} + \frac{2\varepsilon_3}{\alpha_3\lambda_3 - 1} - \frac{2\varepsilon_3^4}{\alpha_3\lambda_3 - 4}\right)\right\} \end{aligned}\right\} \quad (28)$$

Kinetic energy projectile have been entering the soil layer

After the kinetic energy projectile enters the third layer, it penetrates in the single medium. The radial stress on the cavity surface is

$$\left.\begin{aligned} S &= A + B\rho_3 V^2/\tau_{03} \\ A &= \frac{2}{\alpha_3\lambda_3}\varepsilon_3^{-\alpha_3\lambda_3} - \frac{1}{\lambda_3} \\ B &= \frac{6}{(1-\alpha_3\lambda_3)(4-\alpha_3\lambda_3)} + \varepsilon_3^{-\alpha_3\lambda_3} - \frac{2\alpha_3\lambda_3}{1-\alpha_3\lambda_3}\varepsilon_3^{1-\alpha_3\lambda_3} + \frac{2\varepsilon_3^{4-\alpha_3\lambda_3}}{4-\alpha_3\lambda_3} \end{aligned}\right\} \quad (29)$$

It can be seen from the above formula, after the projectile enters the macadam layer medium, *A,B* are related not only to the material characteristics of the three composite media and the thickness of the first two layers, but also to the penetration depth. When kinetic energy projectile penetrates into concrete-macadam-soil composite media, under certain conditions of the results, *A*, *B*, C_A, C_B are functions of penetration depth *L*, while such a situation does not exist when it penetrates into a single medium.

The transformation Eq.(15) is

$$\frac{dV_L}{dL}+\frac{1}{m}C_B(L)\cdot V_L=-\frac{1}{m}C_A(L)V_L^{-1} \quad (30)$$

The above equation is called Bernoulli differential equation, and the relationship between penetration velocity and penetration depth can be obtained by substituting C_A and C_B in different stages into Eq.(30), and then the relationship between acceleration, velocity, penetration depth and time can be obtained.

Pit stage penetration model

When the kinetic energy projectile penetrates into the concrete, due to the interaction between the projectile and the concrete medium, bulges will be formed, and all the concrete in the bulges will be destroyed. The depth from the free surface of concrete to the cylindrical channels is usually defined as the concrete pit depth. For the impact process into a pit, because of the lack of study on failure mechanism, thus in the practical application there is difficult to solve the problem. Considering the impact course is short, the resistance at pit stage penetration can be considered to increase linearly with penetration depth. The resistance acting on the projectile penetration with mass m can be expressed as

$$m\frac{d^2L}{dt^2}=-KL, \qquad 0\le L\le L_c, \qquad 0\le t\le t_c \quad (31)$$

In the formula, K is a constant, L is the instantaneous penetration depth in the pit formation stage, L_c is the pit formation depth, and t_c is the time at the end of the pit formation.

The initial condition is

$$t=0,\quad L=0,\quad V_L=V_0 \quad (32)$$

It can be solved

$$L=V_0\sqrt{\frac{m}{K}}\sin(\sqrt{\frac{K}{m}}t),\quad V_L=V_0\cos(\sqrt{\frac{K}{m}}t) \quad (33)$$

If the effect of composite medium is not taken into account, the following equation can be obtained:

$$V_c^2=\frac{mV_0^2-L_cC_A}{m+L_cC_B} \qquad t_c=\frac{\cos^{-1}(V_c/V_0)}{(K/m)^{1/2}} \qquad K=\frac{m(V_0^2-V_c^2)}{L_c^2} \quad (34)$$

In Eq. (34), V_c and t_c are the velocity and time after the pit formation. C_A, C_B, A, B, are respectively determined by Eq.(13), Eq.(14) and Eq.(29). The pit depth L_c is related to the projectile diameter. It is generally recognized $L_c\cong 4.5r$.

Validation example and discussion

Take the following example, The three-layer target model of the airport runway-Concrete layer 0.65m, macadam layer 0.45m and compacted soil foundation; The steel projectile has a radius of 1.25cm, the quality of 0.505 kg and the initial penetration velocity of 1000m/s. Based on the above analysis, the motion differential equation of penetrating projectile is solved numerically, and the *Runge-Kutta* method is used to calculate the equation. Relevant parameters required in the calculation are shown in Table 1.

Through calculation, the penetration process has the following stages: (1) stage 1- pit forming stage; (2) stage 2- before the elastic-plastic interface reaches the concrete- macadam interface; (3) stage 3-after the elastic-plastic interface reaches the concrete-macadam interface, at this moment, the penetrating projectile has penetrated through the concrete layer; (4) stage 4- penetration projectile enters the macadam layer. The penetration depth, residual velocity and the end time of penetration at each stage are shown in Table 2.

Table-1: Parameters of multi-layer target model and materials

Parameter	value	Parameter	value	Parameter	value
r	$0.0125m$	τ_{01}	$25MPa$	λ_2	0.35
l	$0.06m$	λ_1	0.15	H_2	$1.1m$
R	$0.075m$	H_1	0.65m	ρ_3	$1600kg/m^3$
m	$0.505\ kg$	ρ_2	$1800kg/m^3$	E_3	$0.12GPa$
ρ_1	$2500kg/m^3$	E_2	$10GPa$	τ_{03}	$6MPa$
E_1	$25GPa$	τ_{02}	$10MPa$	λ_3	0.50

Table-2: Parameters calculating values of each penetration phase

Phase	L (m)	V (m/s)	t ($_{\times10^{-3}}$s)
1	0.12	894.7	0.12
2	0.40	506.4	0.53
3	0.65	284.3	1.20
4	0.79	0	2.40

The projectile penetrates the first layer of concrete and then penetrates the macadam. According to the penetration calculation formula for multi-layer media of runway in reference 10, the residual velocity after penetrating the concrete layer is calculated to be 283.39m/s. The above calculation value 284.3m /s is close to this value, indicating that the calculation model and the numerical method have certain reliability in solving the motion equation. In the following research, the residual penetration velocity of other layers will be compared with relevant test data to further improve the calculation model.

The velocity curve obtained by calculation is shown in Fig.4. The velocity curve of penetration in a single concrete medium at the same velocity is also given in Fig.4.

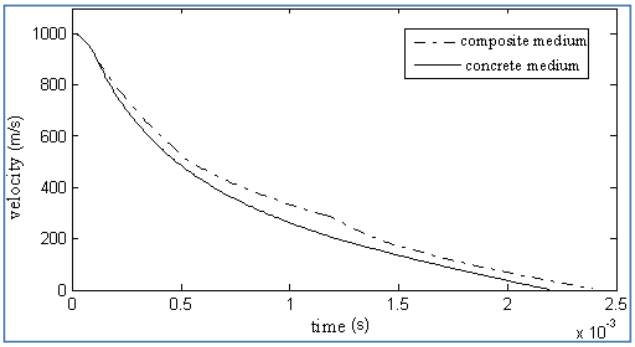

Fig-4: Time-history curve of velocity

It can be seen from the penetration velocity curve that, since the influence of composite medium is not considered in the pit forming stage, the velocity of composite medium and single concrete medium is the same at the pit forming stage, and the velocity change rate achieves the maximum value in the whole penetration process. Before $t=1.2\times10^{-3}$s, penetration projectile moves in the concrete composite medium, and it is noted that the velocity at this time is greater than that in the single concrete medium, and it becomes more and more obvious with the increase of penetration depth. This is mainly because the elastic zone decreases with the increase of penetration depth when penetration projectile penetrates in the composite medium. Due to the influence of the concrete-macadam interface, the pressure in the elastic zone is gradually reduced, and the pressure in the concrete plastic zone is also gradually reduced, so that the resistance is reduced, leading to a gradual decrease in the rate of velocity change.

Numerical model of multi-layer media penetration in runway

By the finite element software ANSYS/LS-DYNA, a three-layer target model of airport runway is established to simulate the penetration process [11-12], as shown in Fig.5. The parameters of each calculated material model are as Table 3 to Table 6.

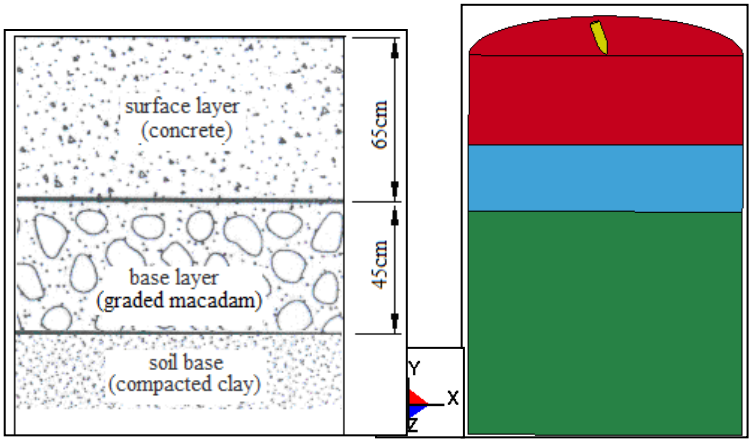

Fig-5: Runway calculation model

Table-3: Projectile material parameters [13] (MAT_JOHNSON_COOK)

ρ/(g/cm3)	G/(GPa)	A/(MPa)	B/(MPa)	n	C	Tm/K
7.8	81.8	792	510	0.26	0.014	1.79

Table-4: Concrete material parameters [14] *(MAT_JOHNSON_HOLMQUIST_CONCRETE)*

ρ/(g/cm3)	G/(GPa)	F_c /(MPa)	T/(MPa)	P_c /(MPa)	μ_c	P_l/(MPa)
2.2	11.9	35	3.67	11.7	0.001	600
μ_l /(MPa)	k_1 /(GPa)	k_2 /(GPa)	k_3/(GPa)			
0.09	85	-171	203			

Table-5: Macadam material parameters [14] *(MAT_JOHNSON_HOLMQUIST_CONCRETE)*

ρ/(g/cm3)	G/(GPa)	F_c /(MPa)	T/(MPa)	P_c /(MPa)	μ_c	P_l /(MPa)
1.8	6.68	20	2.77	6.67	0.001	500
μ_l /(MPa)	k_1 /(GPa)	k_2 /(GPa)	k_3/(GPa)			
0.11	85	-171	203			

Table-6: Soil material parameters [15] *(MAT-SOIL-AND-FOAM)*

ρ /(g/cm³)	μ	E/(MPa)	G/(MPa)	K/(GPa)	a_0	a_1	a_2
1.86	0.48	47.38	16	0.39	2400000Pa²	13600Pa	0.1232

Analysis of penetration process

Fig.6 to Fig.8 clearly show the process of airport runway destruction and the trajectory of projectile penetration by the kinetic energy projectile penetrating at the velocity of 400 m/s, with the incident Angle of 20°. Figure 4 shows the pitting and laminar cracking phenomenon in the process of concrete target penetration, which is due to the fact that concrete is a brittle material containing many defects (micro cracks and micro cavities).And the free surface of the target near the impact point at the instant of impacting makes it prone to form crater fracture area. When the projectile quickly breaks through the concrete target plate, the tensile stress formed on the free surface causes the target plate to crack and form the collapse at the exit.

When the kinetic energy of the projectile is consumed during penetration, the projectile will stay in the target plate.

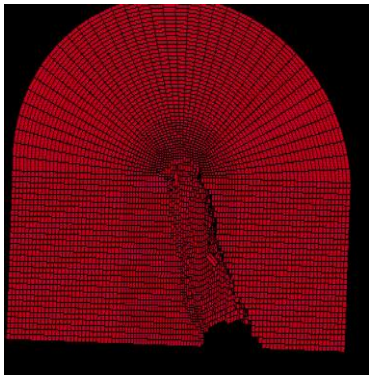

Fig-6: Pits and cracks in the concrete layer

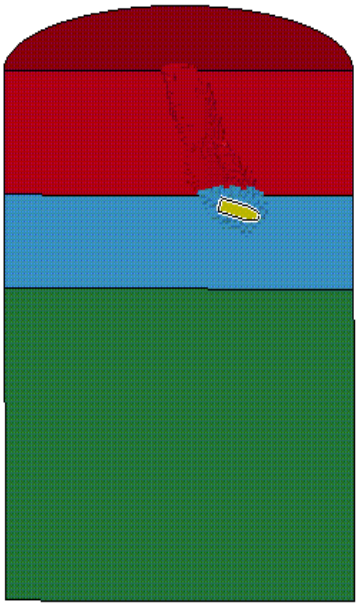

Fig-7: The penetration process

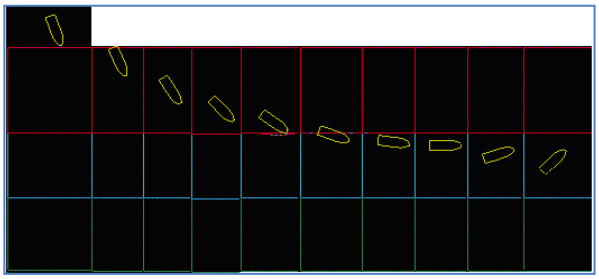

Fig-8: Penetration trajectory (v=400 m/s)

Effects of different velocity on penetration results

The process of kinetic energy projectile penetrating at 600 m/s and incident angle 20° is shown in Fig.9. It can be seen from the Fig.8 and Fig.9 that the presence of multi-layer medium interface accelerates the attitude reversal of the projectile body, and the smaller the penetration speed is, the more obvious the phenomenon will be. This is because when the egg-shaped penetration projectile penetrates into another layer of medium obliquely, it needs to open the pit again. In the opening pit stage, the penetration warhead is subject to great resistance, and the resistance direction is horizontal and upward. As a result, the downward penetration velocity of the tail unit is greater than that of the head unit, and the penetration warhead part slides forward along the interface of the medium, thus increasing the turnover of the projectile shaft. When penetration velocity is small, the whole opening time is longer, that is, the duration of the turning torque is longer, so the influence of the medium interface on the projectile body will be greater.

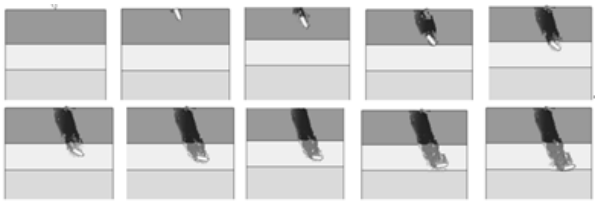

Fig-9: Penetration trajectory *(v=600 m/s)*

Combined with the structural size of the airport runway in the model, it can be seen from Fig.10 that in the whole process of kinetic energy projectile penetrating the runway, there are three obvious overload peaks. The first peak appeared in the concrete pit opening segment of penetration projectile invasion, the second peak appeared in the pit opening segment of penetration projectile invasion compacted macadam layer, and the third peak appeared near the end of penetration. Due to the influence of the interface, after the penetration projectile reaches the interface between the macadam layer and the soil layer, the penetration projectile posture changes greatly, and the penetration resistance area increases rapidly, resulting in the third peak of overload, and then the penetration stops.

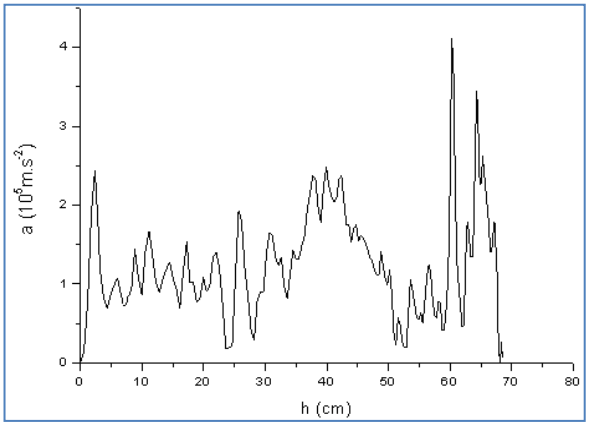

Fig-10: Overload - penetration history curve

The results of numerical analysis are also consistent with the previous theoretical analysis. It is further explained that the trajectory of the projectile mass heart is related to penetration velocity, the properties of the runway medium, penetration depth and other factors. In order to understand the attitude of the projectile body penetrating the multi-layer media in the airfield runway, it is a reliable and effective method to adopt reasonable numerical simulation calculation.

CONCLUSION

Based on the analysis of the penetration process of kinetic energy projectile into the composite media of concrete macadam, the penetration model of kinetic energy projectile into the concrete-macadam-soil composite media is established by using the spherical cavity expansion theory and considering the interface effect. Theory and numerical analysis show that the resistance of kinetic penetration projectile in the movement of concrete layer and macadam layer is not only related to the impact velocity, mass, shape and properties of medium, but also related to penetration depth. Compared with the penetration solution in a single concrete medium, it is noted that the velocity in the composite medium is higher than that in a single concrete medium, and with the increase of penetration depth, it becomes more and more obvious. The three-dimensional numerical simulation shows that the presence of the runway multi-layer dielectric interface accelerates the attitude reversal of the projectile body, and the smaller the penetration speed is, the more obvious the phenomenon will be, and at the same time, the overload response of the projectile body is changed.

The research results lay a foundation for the further research on the composite media penetration technology of airfield runways and have reference value for the research on the damage of civil engineering materials under dynamic load. However, the penetration of composite media is a very complicated mechanical process, which needs further study in theory, numerical calculation and experiment.

ACKNOWLEDGEMENTS

This work is financially supported by National Natural Science Foundation of China (NSFC, 51408057) & Youth Talent Project of Yangtze University (2015cqr06).

REFERENCES

1. Norwood, F.R. (1974). Cylindrical cavity expansion in a locking soil. SLA-74-0201.
2. Forrestal, M.J. (1986). Penetration into dry porous rock. *Int J Solids Struct*, *22*(12):1485–500.
3. Forrestal, M.J., Luk. V.K. (1988). Dynamic spherical cavity expansion in a compressible elastic-plastic solid. *Journal of Applied Mechanics*, *55*(2):275-279.
4. Forrestal, M.J, Frew, D.J. (1996). Penetration of grout and concrete targets with ogive-nose steel projectiles. *Int J Impact Eng*, *18*(5):465-476.
5. Forrestal, M.J, Tzou, D.Y. (1997). A Spherical Cavity-Expansion Penetration Model for Concrete Target. *Int J Solids Struct*, *34*(31/32): 4127-4146.
6. Gao, S.Q., Liu, H.P., Li, K.J. (2006). Normal Expansion Theory for Penetration of a Projectile against Concrete Target. *Applied Mathematics and Mechanics*, *27*(4):431-438.(in Chinese).
7. Wang, Y.B., Yu, M.H., Lin, J.D. (2004). Cylindrical Cavity Expansion Model for Projectile Normally Penetrating into Concrete Target. *Journal of Xi'an Traffic University*, *38*(3):303-307.(in Chinese)
8. Lin, J.X., Jiang, H.Z., Jiang, J. (1999). An Analytical Model for Projectile Normally Penetrating into Layered Target of Soil/Concrete. *Journal of Ballistics*, *11*(1):1-10.(in Chinese)
9. Chaomei, M., Qinghua, T., Zhigang, J. (2018). Approximate solutions of finite dynamic spherical cavity-expansion models for penetration into elastically confined concrete targets. *International Journal of Impact Engineering*. (114):182–193.
10. Wang, D.H., Jiang, L.J. (1993). Study on Penetration of Projectile into Multilayer Medium Runway. *Journal of Projectiles, Rockets, Missiles and Guidance*, (3): 46-54.(in Chinese)
11. Xu, W.F., Huang, X.C., Hao, Z.M. (2011). Parametric Studies on the Penetration of KE-projectile into Airstrip. *Chinese Journal of Applied Mechanics*, *28*(4): 443-446.(in Chinese)
12. Li, W.P., Sun, H., Shuai, G.H. (2012). Engineering Arithmetic of Kinetic Projectile Penetrating Airport Runway. *Ordnance Material Science and Engineering*, *35*(2):12-15.(in Chinese)
13. Zeng, B.Q., Jiang, C.L., Wang, Z.C. (2007). 3D Numerical Simulation of Oblique Penetration of Antirunway Penetrator to a Multilayer Runway Target. *Acta Armamentaril*, *28*(12):1433-1437. (in Chinese)
14. Zhang, F.G., Li, E.Z. (2001). A Method to Determine the Parameters of the Model for Concrete Impact and Damage. *Journal of Ballistics*, *13*(4):12-16. (in Chinese)
15. Forrestal, M.J., Luk, V.K. (1992). Penetration into soil targets. *Int J Impact Eng*, *12*(5):427-444.